# Optimization of Plasmonic Heating by Gold Nanospheres and Nanoshells

*Nadine Harris, Michael J. Ford* and Michael B. Cortie*

Institute for Nanoscale Technology, University of Technology, Sydney, NSW, 2007.

*Corresponding author: Mike.Ford@uts.edu.au

Gold nanoparticles have strong and tunable absorption peaks in their optical extinction spectra, a phenomenon that has recently been exploited to generate localized heating in the vicinity of these particles. However the optimum particle geometry and illumination regime to maximize these effects appears not to have been previously examined in any detail. Here we show that the interplay between the particles' absorption cross-sections, volume and surface area lead to there being specific conditions that can maximize particle temperature and surface heat flux. Optical absorption efficiencies were calculated from the formulation of Mie, and radiative, convective and conductive heat transfer models used to model the thermal performance of particles in different situations. Two technologically relevant scenarios for illumination, namely irradiation by sunlight at 800 $W/m^2$, and by a monochromatic laser source of 50 $kW/m^2$ tuned to the peak absorption wavelength, were considered. For irradiation by sunlight, the resultant heat flux is optimized for an 80 nm diameter nanoshell with an aspect ratio of 0.800, while for irradiation by laser the maximum heat flux is found for 50 nm nanoshells, with an aspect ratio of 0.9. The optimum for solid nanospheres is at 110 nm for sunlight and 80 nm in monochromatic illumination tuned to the absorption maximum.

**Keywords:** temperature, localized, laser, convection, conduction, radiation.

## 1. INTRODUCTION

The absorption and scattering of light by nanoparticles, particularly those made of gold, has received considerable attention in recent years. The interest lies in the unusually large absorption cross-sections, which are much larger than the geometric cross-sections, at wavelengths corresponding to surface modes in the particle. Moreover, it has been shown how these surface modes can be tuned over a wide wavelength range by using, for example, gold 'nanoshells' of varying thickness [1-3] (these particles are also known as 'core-shell' particles *e.g.*[4,5]). A variety of therapeutic applications for this phenomenon are being explored which exploit the temperature change induced by the strong plasmon-induced surface heat flux of nanoshells or nanospheres[6]. Considerable progress in respect of drug release[7,8] and targeted hyperthermal destruction of tumor cells[9-12] using nanoshells has been made by the group of N. Halas in the USA, although some success in these respects has also been achieved by other groups with ordinary gold nanospheres[13-15]. There have been several fundamental studies of the phenomena occurring during the laser-induced heating of gold nanospheres *e.g.*[16-18] but only a very few such studies for gold nanoshells, *e.g.*[19].

The relationship between optical extinction spectra and nanoshell or nanosphere geometry is now well established. However, while temperature changes as a result of incident illumination have been calculated[4,13,18] and/or measured[4,9,18,20] for these particles, there is an important aspect of their behavior that has been neglected; this is that the magnitude of the heat flux off their surfaces and the details of the associated temperature profiles in the surrounding media are optimized for certain special geometries and controlled by the nature of the heat transfer taking place. Here we explore these effects. We maintain that an understanding of these interactions is essential in order to properly exploit plasmonic heating in these particles.

## 2. METHOD

### *2.1 Calculation of Absorption Efficiency and Heat Flux*

The computer program BHCOAT described by Bohren and Huffman, was used to calculate scattering from the nanoshells [21]. BHCOAT calculates scattering by using Mie Theory [22] to provide numerical solutions for scattering efficiency, $Q_{sca}$ (scattering cross-section, $C_{sca}$ divided by geometric cross-sectional area), absorption efficiency, $Q_{abs}$ (absorption cross-section, $C_{abs}$ divided by cross-sectional area), and extinction efficiency, $Q_{ext}$ ($Q_{ext} = Q_{sca} + Q_{sca}$). In principle this is an exact solution to the scattering problem for spheres. In practice, however, the infinite multipole expansion must be terminated at some point and the exactness of solution is therefore determined by how quickly this series converges. For spheres that are small compared to the wavelength of the incident light only the first one or two terms of the expansion (the dipole and quadrupole terms) make a significant contribution. Even for the largest particle sizes investigated here series convergence is not expected to be a problem. More problematic in BHCOAT is the calculation of potentially very large numbers. The scattering coefficients cannot be written in such a way that functions of complex arguments are ratios as they can for the solutions for solid spheres. This can lead to numerical problems if the shell is particularly large or absorbing, that is, has a large imaginary component of the refractive index. A rough guide given by the authors of BHCOAT is that the imaginary component of the size factor times shell radius for inner or outer shell should not exceed about 30. For the largest shells in this work we are approaching this limit, with maximum values of about 10. To determine whether our calculated scattering efficiencies are subject to these numerical problems we have compared calculations for solid spheres using the BHCOAT algorithm, where the inner and outer sphere are composed of the same material, to calculations using the BHMIE algorithm from Bohren and Huffman [21] which is the exact solution for a solid sphere. The latter does not suffer with the numerical problems described above, any difference between the two methods is therefore an indication of numerical problems in BHCOAT. For all particle sizes the two algorithms give identical results.

Nanoshells with diameters of 30 nm, 50 nm, 80 nm, 110 nm, 200 nm, 250 nm, 300 nm, 350 nm and 400 nm with aspect ratios of 0, 0.2, 0.4, 0.6, 0.8, 0.85, 0.9, 0.925 and 0.95 were simulated. The aspect ratio is the ratio of the inner sphere diameter to the outer shell diameter. An aspect ratio of 0 describes a solid gold sphere, and a 0.95 aspect ratio is one where the shell thickness is 5 % of the diameter of the sphere. The nanoshells were simulated as a suspension in water (with the water also making up the core of the nanoshell) by modifying the frequency dependent refractive index of bulk gold (taken from [23]) so that it is relative to water. The refractive index of water was taken to be frequency independent and non-absorbing. This is justified as the value of refractive index varies by only 2% across the spectrum investigated here [24]. Calculations were performed on each nanoshell between wavelengths of 300 nm and 1500 nm in 1 nm increments. This range of wavelengths was chosen as they include the surface modes for all particle geometries and hence include the dominant absorption bands.

Assuming that all the energy absorbed from the incident light is converted to thermal energy, then under steady-state conditions the power absorbed by (and of course simultaneously transferred out of) a single particle is

$$\dot{Q} = \int_{300}^{1500} C_{abs} E_{\lambda} .d\lambda \qquad (1)$$

and the surface heat flux is

$$\dot{q} = \frac{1}{4} \int_{300}^{1500} Q_{abs} E_{\lambda} .d\lambda \qquad (2)$$

where $\dot{Q}$ is the heat transfer rate (W), $C_{\text{abs}}$ the absorption cross section, $E_{\lambda}$ is the spectral irradiance of the light source ($W.m^{-2}.nm^{-1}$), $\lambda$ the wavelength of light, and $\dot{q}$ the heat flux ($W/m^2$) at the nanoparticle surface (the nomenclature used in standard texts has been followed here[25,26]). Temperature-induced bleaching[18] of the plasmon resonance has been neglected. Two scenarios were considered for the incident radiation. The first was to simulate irradiation of the nanoshells in 800 $W/m^2$ of standardized sunlight[25]. The second was to simulate irradiation of the nanoshells by a 10 mW continuous wave laser with a 0.5 mm diameter spot size (giving 50.9 $kW/m^2$). It was assumed that the wavelength of this laser

could be tuned to the wavelength of maximum absorption of the nanoshells. These sources of irradiation correspond to two potential applications of plasmonic effects in nanoparticles: wavelength selective solar glazing, and localized heating under laser irradiation for therapeutic treatment. There are also two very different scenarios for the laser illumination, and various possible situations with regard to the mechanism of heat transfer; these are that the illumination times can be sufficiently long so as to equilibrate the particles with the fluid, or they might be so short that transient effects occur in the particles and/or surrounding medium and, that the particles might be suspended in a fluid, or immobilized in a gelatinous or solid matrix.

### *2.2 Relationship of Heat Flux to Particle Temperature*

Past work[13,18] on transient heating and cooling has focused on the temperature of the particle itself. However, this is something of a red herring. It is not the high temperature of the particle that would cause it to have functionality in, for example, a therapeutic application. Rather, it is the temperature that the particle imparts to its immediate surroundings. This is completely determined by $\dot{q}$. However, once the surface heat flux $\dot{q}$ is known, the steady-state particle temperature can be estimated, if desired, using a model that accounts for heat loss by a suitable mechanism.

The maximum particle temperature would be achieved when heat loss is by radiation alone since this is a relatively ineffective mechanism at temperatures below 1000K; the minimum particle temperature will result if heat loss from the particle over short times is by conduction, since this initially imposes the temperature of the bulk medium directly onto the surface of the gold[18]. Heat transfer will always be very high and virtually at conductive levels in the first microsecond of illumination when the hot particle is in contact with a cold medium but as the energy produced by the particle flows into the surrounding medium to produce a boundary layer of warm fluid, the discrepancy between predictions by the conductive and convective mechanisms is rapidly increased. The convective mechanism will become dominant after about one second if buoyancy-induced displacements of the fluid or the nanoparticles entrained in the fluid take place. In this case, once steady state is achieved, a large proportion of the

thermal energy will be carried by mass transfer, and convection will be a more significant factor than conduction. However, if the particles and their surrounding medium are immobile then heat transfer by conduction alone will continue to operate.

The equilibrium temperature due to radiative cooling alone can be calculated by setting the absorbed power equal to that radiated by a black body at temperature $T_p$ [27]

$$\dot{Q} = e\sigma 4\pi r_p^2 (T_p^4 - T_{surr}^4) \qquad (3)$$

where $e$ is the emissivity of the nanoshell ($e = 0.9$ for nanoparticulate gold), $\sigma$ is Boltzmann's constant, $r_p$ is the radius of the nanoshell, $T_p$ is the temperature of the nanoshell and $T_{surr}$ is the ambient temperature of the surroundings[27]. Since $\dot{Q}$ can be calculated from Equ.(1), $T_\mathrm{p}$ can be extracted in this case.

Calculation here of the thermal conditions around a particle subject only to conductive heat transfer made use of the Goldenberg-Tranter model for a heat-generating sphere in an infinite conductive medium[28], which is available in an accessible (and corrected) version due to Pitsillides et al.[13]**.** Details of the model and its implementation here are given in the Supporting Information.

Estimation of $T_\mathrm{p}$ in the case of convective heat transfer is more troublesome. The efficiency of heat transfer across the interface in this case is parameterized by a heat transfer coefficient, *h*. Here we assume also that the total amount of heat transfer, *Q*, of the experiment was sufficiently small so as not to make a significant change to the temperature of the bulk fluid and that time scales are sufficiently long so as to allow buoyancy-induced mass transfer to take place. The nanoparticles are assumed to be a sufficiently dilute suspension that they do not interact with one another either thermally or plasmonically. The rate of heat transfer due to convection can then be described by[27]

$$\dot{Q} = h4\pi r_p^2 (T_p - T_{surr}) \qquad (4)$$

However, the difficulty still lies in finding an appropriate value for *h*. There is no *a priori* reason why the well-known macroscopic empirical data for *h* would apply at the nanoscale. Values of *h* in steady state macroscopic aqueous systems water range[26] from 50 to 10,000 W/m$^2$/K, but are orders of

magnitude higher at the initiation of heating transients[26]. In practice the value of $h$ in novel situations is generally determined by experiment. For this reason we have presented results for two values of $h_{con}$; 500 W/m$^2$/K (applicable to free convection in still water, the situation that might apply in a dilute suspension after several seconds of heating), and 10,000 W/m$^2$/K (applicable to very short heating times and before the thermal boundary layer is fully established).

## 3. RESULTS

### *3.1 Optimum particle geometries*

The aspect ratio of a nanoshell is the dominating influence on the wavelength at which maximum absorption occurs[3]. However, for a fixed aspect ratio, the wavelength at which maximum absorption occurs nevertheless also shows some dependence on shell diameter. As the shell diameter increases the peak broadens due to contribution of higher order terms to absorption and scattering. The efficiency at the absorption peak is also size dependent; larger shells tend to scatter incident light more efficiently and absorb less compared with smaller diameters [29]. This can be seen in Figure 1 where absorption and scattering of 80 nm and 400 nm diameter solid-core spheres are compared. An 80 nm diameter sphere absorbs approximately 2.5 times the amount it scatters, whereas a 400 nm diameter sphere scatters approximately 2.5 times the amount it absorbs.

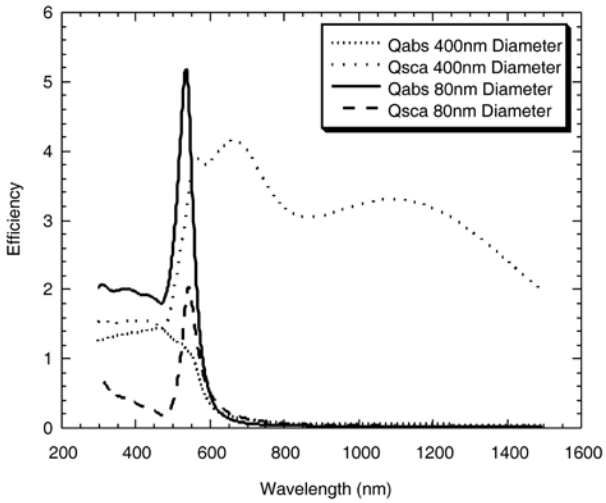

**Figure 1.** Absorption Efficiency, $Q_{abs}$, and Scattering Efficiency, $Q_{sca}$, for 80 nm and 400 nm nanospheres (aspect ratio=0).

The peak absorption efficiencies as a function of nanoshell diameter for fixed aspect ratios are shown in Figure 2. The optimum absorption efficiency of $Q_{abs} \approx 19$ occurs at a diameter of 50 nm and aspect ratio of 0.9. For a solid sphere of the same diameter the peak absorption efficiency is almost a factor of 5 smaller, $Q_{abs} \approx 4$. For all aspect ratios the absorption efficiency falls rapidly beyond shell diameters of about 100 nm, because these larger particles scatter more efficiently.

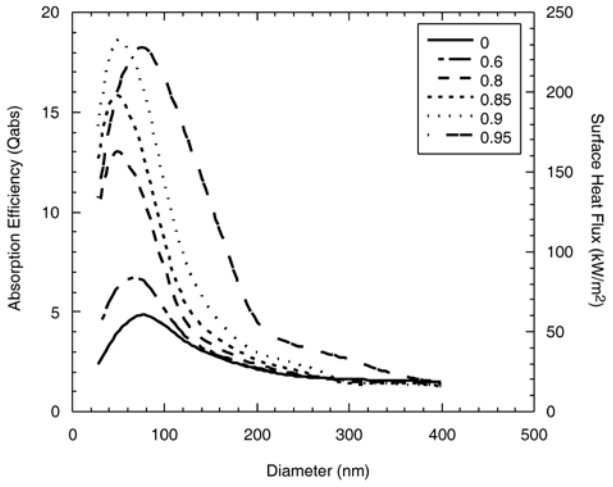


**Figure 2.** Peak absorption efficiencies, $Q_{abs}$ as a function of nanoshell diameter for fixed aspect ratios, and associated surface heat flux.

From Equation (2) the surface heat flux under the laser radiation is in direct proportion to $Q_{\text{abs}}$ , and can therefore also be shown in Figure 2. It can be seen that the 50 nm, 0.9 aspect ratio nanoshell produced a maximum surface heat flux of 245 $kW/m^2$ as compared to the maximum 50 $kW/m^2$ surface heat flux produced by nanospheres, of about the same diameter. In this case the optimum geometry is the same as that which produced the maximum absorption. The situation is a little different in sunlight, Figure 3. The maximum surface heat flux of approximately 175 $W/m^2$ occurs for a diameter of 80 nm and an aspect ratio of 0.800. Note that the optimum surface heat flux, in this case, does not correspond

to an aspect ratio that gives the optimum absorption efficiency. Also, a solid sphere of diameter 110 nm gives a nearly comparable surface heat flux, 150 $W/m^2$. This effect occurs because the wavelength position of the absorption maximum is strongly dependent upon aspect ratio, whereas the maximum irradiance of the incident radiation is fixed.

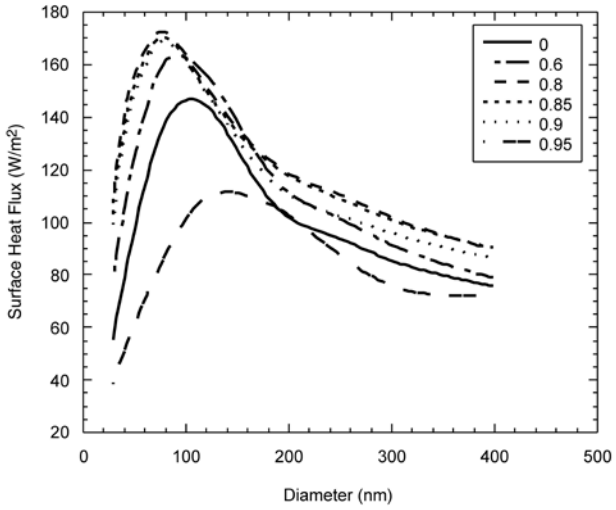


**Figure 3.** Variation of surface heat flux versus nanoshell diameter for fixed aspect ratios when irradiated with sunlight.

Figure 4 shows the variation of the absorption peak as a function of aspect ratio for 50 nm diameter shells. For the solid sphere the absorption maximum occurs at about 530 nm whereas for the 0.9 aspect ratio shell it is at 846 nm. Since the majority of the Sun's intensity falls between about 400 nm and 700 nm [27], thicker shells, that is those with a smaller aspect ratio and diameter are best suited to converting sunlight to heat flux. However, proposed therapeutic applications, which use monochromatic radiation in the near infra-red, are best served by shells of aspect ratios of 0.9 to 0.95.

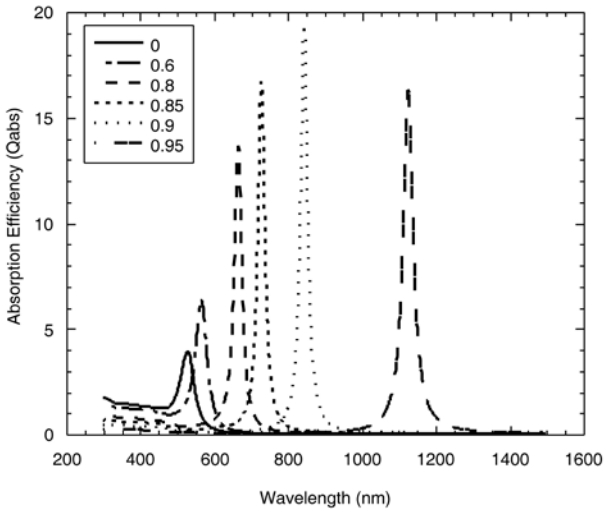


**Figure 4.** Absorption Efficiencies for a 50 nm diameter nanoshell with varying aspect ratios.

While the surface heat flux is an important criterion, it is instructive to also consider the situation when $\dot{Q}$ is normalized against the mass of gold in the particle, Figure 5. In this case the smaller the particle, the more efficient its coupling with light. In addition, the increased $Q_{abs}$ and smaller gold content of the high aspect ratio shells more than compensates for the shift in wavelength of their maximum absorbance to the infra-red. If maximum heat generation with lowest possible gold loading is needed, then shells of the highest practicable aspect ratio and smallest diameter are indicated.

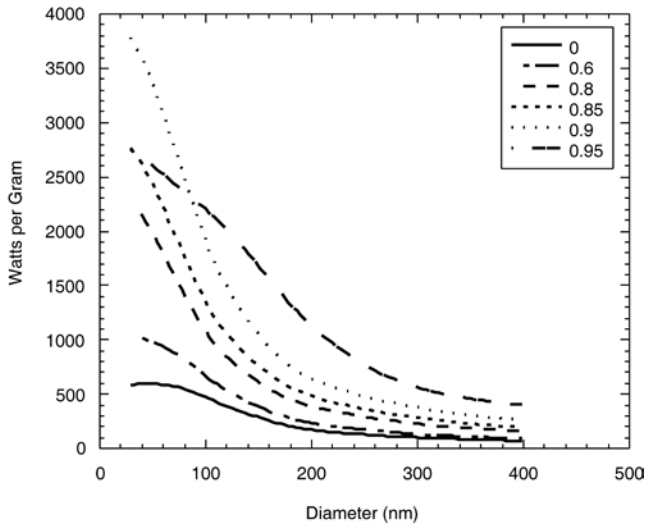


.

(a)

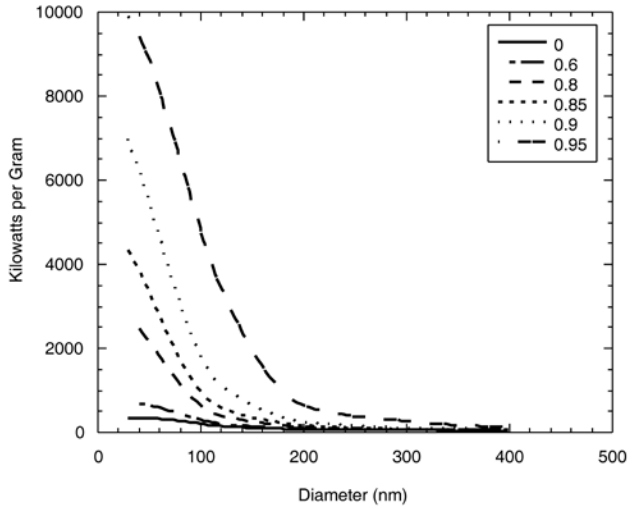


(b)

**Figure 5.** Efficiency of heat generation expressed in terms of mass of gold required, (a) in sunlight, (b) under monochromatic laser illumination at 50.9 kW/m$^2$

### *3.2 Heat transfer by radiation*

As mentioned, the maximum particle temperatures would be achieved if heat transfer was by radiation alone. The equilibrium temperature for the gold nanoshells in vacuum where the surroundings are at ambient temperature (293 K) is given in Figure 6. Under illumination by sunlight the maximum equilibrium temperature of 535 K is reached for an 80 nm nanoshell with an aspect ratio of 0.800. However, under the laser illumination a maximum equilibrium temperature of 1775 K occurs for the 50 nm diameter nanoshell with an aspect ratio of 0.9. In this case the optimum geometry directly matches the results of the heat flux calculations in the preceding section. Obviously, both the ability to tune the laser wavelength to the peak absorption wavelength, and the higher fluence of the laser, give a much larger final temperature. No account is taken in this calculation of melting of the nanoshell, which is known to occur under sufficiently intense laser illumination[19].

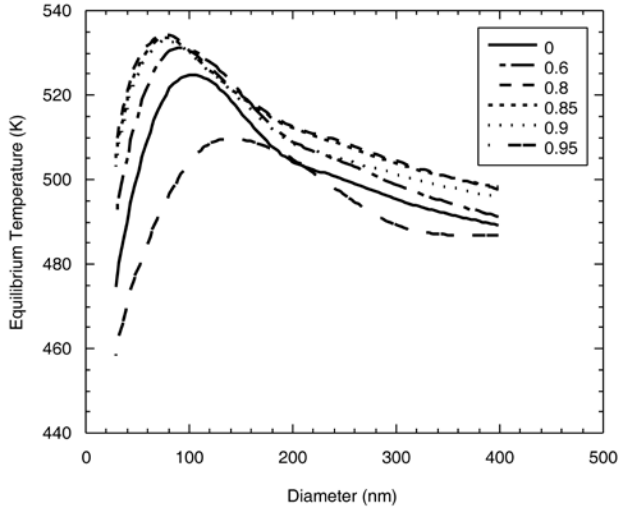


(a)

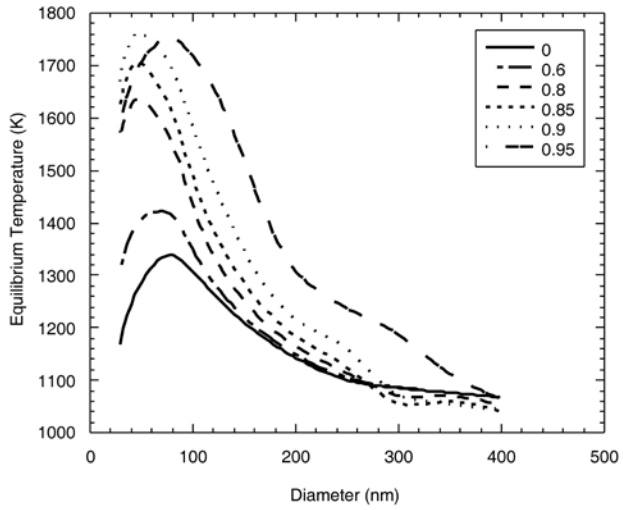


(b)

**Figure 6.** Nanoshell equilibrium temperature after irradiation in vacuum, (a) sunlight and (b) monochromatic laser.

### *3.3 Transient effects due to pulsed irradiation*

Application of very short (femtosecond to nanosecond), high power laser pulses produce rapid heating in a nanoparticle[13,18], followed shortly thereafter by rapid cooling[18] when the laser radiation ends. In this

scenario mass transfer of water or particle does not take place within the time frame of the experiment due to inertial considerations. The mechanism of heat transfer out of the particle can therefore be taken as conductive[13,18]. Negligible effects take place in sunlight within this ultra-short time domain, but the effects are significant in the case of the laser illumination. Simulations of the temperature within particle and medium at the end of single laser pulses of varying duration are shown in Figure 7. The effect of increasing the duration of the pulse is to increase the diameter of the bubble of warm water around the particle, but at the expense of a rapidly increasing particle temperature. We will return in the Discussion section to this effect.

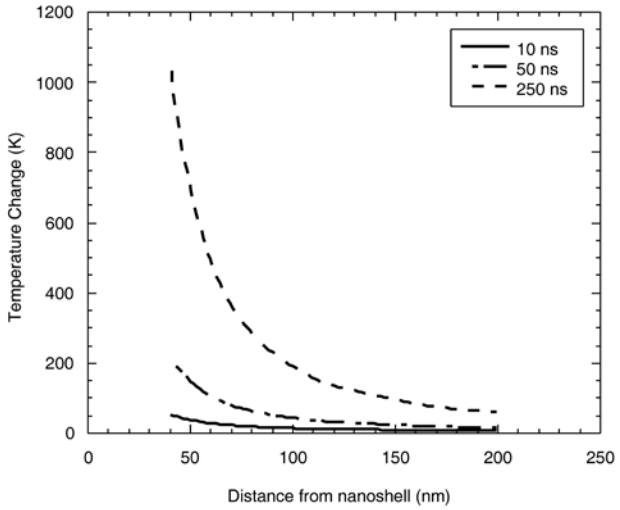


**Figure 7.** Calculated temperature rise profiles in vicinity of gold nanoshells subjected to monochromatic laser radiation at 50.9 kW/m$^2$ for the indicated time.

### *3.4 Continuous irradiation in water*

The resultant equilibrium temperatures for nanoshells suspended in water and irradiated in sunlight are shown in Figure 8 for an assumed $h$=500 W/m$^2$/K. In Figure 9 we show the situation for laser irradiation and $h$ values of 500 W/m$^2$/K. (corresponding to of over 1 second in water) and 10,000 W/m$^2$/K (corresponding to exposures of in the order of microseconds).

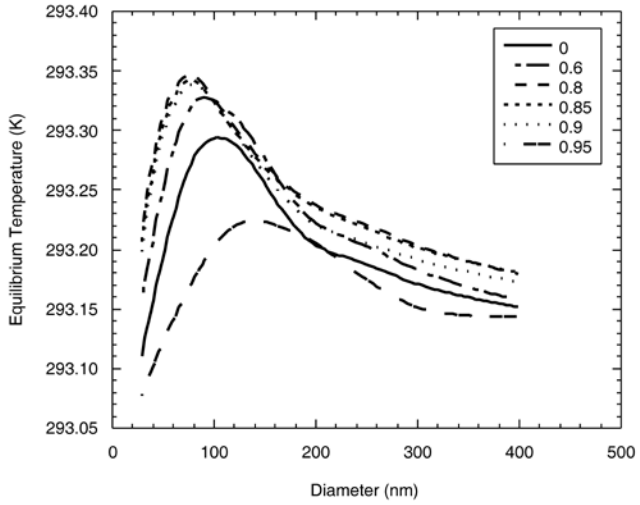


**Figure 8.** Nanoshell equilibrium temperature after irradiation with sunlight while immersed in a water medium with $h$=500 W/m$^2$/K.

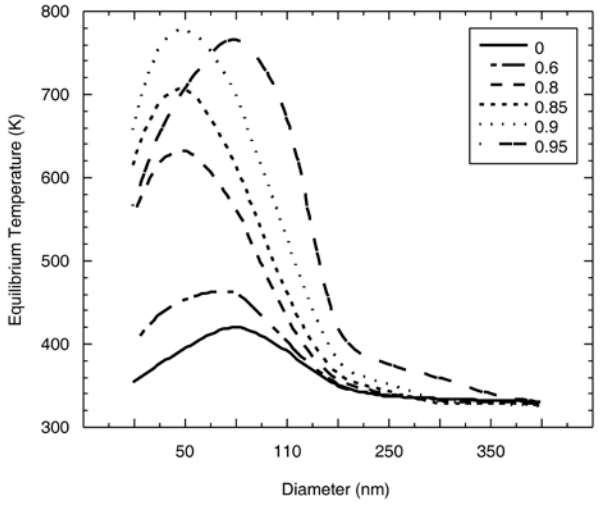


(a)

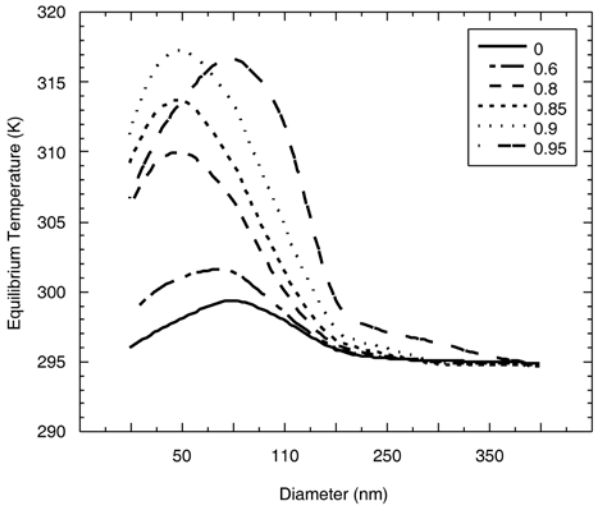


(b)

**Figure 9.** Nanoshell equilibrium temperature after irradiation with laser at 50.9 kW/m$^2$ while immersed in a water medium (a) corresponds to $h$=500 W/m$^2$/K and (b) to $h$=10,000 W/m$^2$/K.

As expected, the optimum geometries for maximum equilibrium temperature again follow directly from the trends found for $Q_{abs}$ and heat flux. Under sunlight there is negligible temperature change, the maximum equilibrium temperature being only 293.35 K for the 80 nm diameter, 0.8 aspect ratio nanoshell. By comparison, when illuminated by the laser light the 50 nm diameter, 0.9 aspect ratio shell would reach an equilibrium temperature of 790 K when suspended in water under conditions that gave $h$=500 W/m$^2$/K, and 318 K when suspended in water with $h$=10,000 W/m$^2$/K.

## 4. DISCUSSION

It is clear that the different geometries of nanoshell are not the same when it comes to generating localized heat fluxes. We have shown here that, irrespective of the magnitude of the applicable heat transfer coefficient, the optimum nanoshell under conditions of laser irradiation has a diameter of 50 nm and an aspect ratio of 0.9. This shape provides the highest possible heat flux, and we suggest that it would be a most appropriate shape for applications that require plasmonic heating. In water this

particular shell has a calculated absorption maximum at 846 nm, which is well positioned within the so-called 'infra-red window' of human tissue. If the dielectric core were made of polystyrene as opposed to water it would have the effect of red-shifting the peak position and decreasing $Q_{abs.}$

Although it is the heat flux $\dot{q}$ that is ultimately responsible for influencing the environment of the particle, nevertheless the temperatures achieved by the particles themselves will always be of interest, making a closer analysis of the applicable $h$ desirable. As noted previously, $h$ at the instant at which laser illumination starts is very large but it will decline rapidly as an envelope of warm fluid builds up around the nanoparticle. This will cause the temperature of the particle to rapidly rise. At some point the temperature of the fluid immediately adjacent to the particle might become high enough to nucleate vaporization of the fluid. This will occur at a temperature considerably higher than the normal boiling point of water, due to the necessity to nucleate a bubble, but nevertheless below the critical point temperature of water, which is 641 K. In any event, the heat transfer coefficient will fall further once vaporization of the surrounding fluid occurs ($h$ being considerably smaller in vapor than in liquid), and the temperature of the particle will consequently break away to very high values[19]. Under these conditions melting of the gold and fragmentation of the nanoparticle is likely; a phenomenon already demonstrated in diverse experimental studies[13,19,30].

It is possible to optimize the irradiation parameters in order to prevent this situation. If, for example, it is deemed that the temperature of the gold particle should not exceed 641K (or some other necessary limiting temperature) then there is only a limited combination of laser fluences and irradiation durations that can ensure this for a given particle geometry. An analysis for the transient situation as it appears to apply to a 50 nm diameter gold nanoshells of 0.9 aspect ratio is shown in Figure 10. It is expected that conductive heat transfer applies only for very short heating transients, certainly of not more than $1x10^{-4}$ s duration. At longer times convective heat transfer is expected in fluid media, and its associated mass transfer will accelerate the rate of heat extraction from the particle and prolong the time required to reach the target particle temperature. This is shown by the dotted line in the Figure. Similar analyses can obviously be performed for particle geometries.

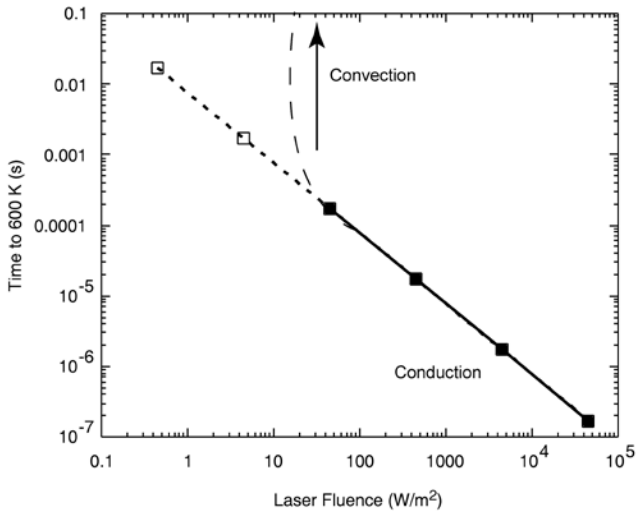


**Figure 10.** Calculated laser fluences and irradiation times to produce a maximum temperature of 640 K in a 50 nm diameter gold nanoshell with aspect ratio of 0.9 under conditions of non-steady state heat conduction. The times will be increasingly under-estimated as convective heat transfer sets in.

## 5. CONCLUSIONS

We have shown that the geometry of nanoshells can be engineered to achieve an maximum surface heat flux. We simulated irradiating the nanoshells via two methods, firstly by 800 $W/m^2$ of sunlight and secondly by a 10 mW, 0.5 mm diameter spot size laser. The absorption efficiency of the particles and hence surface heat flux was calculated from an exact solution to the scattering problem within Mie theory. Equilibrium temperatures for irradiated shells suspended in media with various heat transfer properties were calculated using radiative, conductive and convective heat transfer models.

For nanoshells irradiated by sunlight we found that relatively thick shells with a diameter in the range of 80 nm to 100 nm gave the optimum surface heat flux. Despite the shift in wavelength of the absorption maximum the use of thick shells compared with solid spheres has only a small effect upon the surface heat flux. Nanoshells of 80 nm diameter and 0.8 aspect ratio give the calculated maximum of approximately 175 $W/m^2$. By comparison 110 nm solid shells give a surface heat flux of almost 150 $W/m^2$. When these shells are suspended in water the corresponding equilibrium temperature is essentially the same as the surrounding medium, that is, there is virtually no temperature rise. The

relative insensitivity to the use of shells or solid spheres arises from the broad spectrum of the irradiating sunlight.

Not surprisingly, nanoshells offer dramatic advantages over solid shells when illuminated by a laser source where the laser wavelength can be tuned to the absorption maximum. The calculated maximum surface heat flux in this case occurs with 50 nm diameter, 0.9 aspect ratio nanoshells. For an incident intensity of 10 mW over a 0.5 mm spot size, the value is approximately 245 $kW/m^2$. By comparison, solid spheres give a maximum of only about 50 $kW/m^2$. The corresponding temperature of the particles and surrounding fluid depends on the applicable mechanism of heat transfer. For isolated shells suspended in water under convective conditions the equilibrium temperature in this case is estimated to be about 790 K, a condition reached when the illumination is applied at a wavelength of close to 850 nm.

**ACKNOWLEDGMENT**

This work was supported by the Australian Research Council and the University of Technology, Sydney. Computing facilities were provided by the Australian Center for Advanced Computing and Communication in New South Wales, and the National Facility at the Australian Partnership for Advanced Computing.

**Supporting Information Available**. A description of the heat transfer model used to describe conductive heat dissipation around a nanoparticle while embedded within an infinite homogeneous medium [13]. This material is available free to charge via the Internet at http://pubs.acs.org.

**REFERENCES**

(1) Kerker, M.; Blatchford, C. G. *Physical Review B* **1982**, *26*, 4052.

(2) Neeves, A. E.; Birnboim, M. H. *J. Opt. Soc. Am. B* **1989**, *6*, 787.

(3) Oldenburg, S. J.; Averitt, R. D.; Westcott, S. L.; Halas, N. J. *Chem. Phys. Lett.* **1998**, *288*, 243.

(4) Skirtach, A. G.; Dejugnat, C.; Braun, D.; Susha, A. S.; Rogach, A. L.; Parak, W. J.; Mohwald, H.; Sukhorukov, G. B. *Nano Letters* **2005**, *5*, 1371

(5) Graf, C.; van Blaaderen, A. *Langmuir* **2002**, *18*, 524.

(6) Pissuwan, D.; Valenzuela, S.; Cortie, M. B. *Trends in Biotechnology* **2006**.

(7) Sershen, S. R.; Westcott, S. L.; Halas, N. J.; West, J. L. *J. Biomed. Mater. Res.* **2000**, *51*, 293.

(8) West, J. L.; Halas, N. J. *Current Opinion in Biotechnology* **2000**, *11*, 215

(9) Hirsch, L. R.; Stafford, R. J.; Bankson, J. A.; Sershen, S. R.; Rivera, B.; Price, R. E.; Hazle, J. D.; Halas, N. J.; West, J. L. *Proceedings of the National Academy of Sciences* **2003**, *100*, 13549

(10) West, J. L.; Halas, N. J. *Annu. Rev. Biomed. Eng* **2003**, *5*, 285.

(11) O'Neal, D. P.; Hirsch, L. R.; Halas, N. J.; Payne, J. D.; West, J. L. *Cancer Letters* **2004**, *209*, 171.

(12) Loo, C.; Lin, A.; Hirsch, L.; Lee, M. H.; Barton, J.; Halas, N.; West, J.; Drezek, R. *Technology in Cancer Research & Treatment* **2004**, *3*, 33.

(13) Pitsillides, C. M.; Joe, E. K.; Wei, X.; Anderson, R. R.; Lin, C. P. *Biophysical Journal* **2003**, *84*, 4023

(14) Angelatos, A. S.; Radt, B.; Caruso, F. *Journal of Phys. Chem. B* **2005**, *109*, 3071.

(15) Lapotko, D.; Lukianova, E.; Shnip, A.; Zheltov, G.; Potapnev, M.; Savitskty, V.; Klimovich, O.; Oraevsky, A. *Proceedings of SPIE* **2005**, *5697*, 82.

(16) Mohamed, M. B.; Ahmadi, T. S.; Link, S.; Braun, M.; El-Sayed, M. A. *Chem. Phys. Letters* **2001**, *343*, 55

(17) Hu, M.; Petrova, H.; Hartland, G. V. *Chem. Phys. Letters* **2004**, *391*, 220

(18) Hu, M.; Hartland, G. V. *J. Phys. Chem. B* **2002**, *106*, 7029

(19) Prasad, V.; Mikhailovsky, A.; Zasadzinski, J. A. *Langmuir* **2005**, *21*, 7528

(20) Chou, C.-H.; Chen, C.-D.; Wang, C. R. C. *J. Phys. Chem. B* **2005**, *109*, 11135.

(21) Bohren, C. F.; Huffman, D. R. *Absorption and Scattering of Light by Small Particles*; Wiley: New York, 1998.

(22) Mie, G. *Ann. Physik* **1908**, *4*, 377

(23) Weaver, J. H.; Frederikse, H. P. R. *Optical Properties of Selected Elements*, 82 ed.; CRC Press: Boca Raton, 2001.

(24) Djurisic, A. B.; Stanic, B. V. *Applied Optics* **1999**, *38*, 11

(25) ASTM G159-98. Standard Tables for References Solar Spectral Irradiance at Air Mass 1.5: Direct Normal and Hemispherical for a 37° Tilted Surface1; American Society for Testing and Materials (ASTM), 1998.

(26) Cengel, Y. A. *Heat Transfer. A Practical Approach*; McGraw-Hill: Boston, 1998.

(27) Young, H. D.; Freedman, R. A. *University Physics with Modern Physics*; Addison Wesley Longman Inc, 2000.

(28) Goldenberg, H.; Tranter, C. J. *British Journal of Applied Physics* **1952**, *3*, 296

(29) Schelm, S.; Smith, G. B. *J. Opt. Soc. Am. A* **2005**, *22*, 1288.

(30) Link, S.; Burda, C.; Nikoobakht, B.; El-Sayed, M. A. *Chemical Physics Letters* **1999**, *315*, 12.